

POST PRINT

<https://www.sciencedirect.com/science/article/pii/S0048969716314486>

<https://doi.org/10.1016/j.scitotenv.2016.07.005>

Elsevier Editorial System(tm) for Science of
the Total Environment

Manuscript Draft

Manuscript Number:

Title: Seawater intrusion in karst, coastal aquifers: current challenges and future scenarios in the Taranto area (southern Italy)

Article Type: SI: Integrated Water Manageme

Keywords: saltwater intrusion, karst coastal aquifers, Mediterranean area, sensitivity analysis, groundwater management

Corresponding Author: Dr. Giovanna De Filippis,

Corresponding Author's Institution: Scuola Superiore Sant'Anna

First Author: Giovanna De Filippis

Order of Authors: Giovanna De Filippis; Laura Foglia; Mauro Giudici; Steffen Mehl; Stefano Margiotta; Sergio Negri

Abstract: Arid and semi-arid regions in the Mediterranean area are characterized by very complex hydrogeological systems, about which limited knowledge is available due to the lack of data. Furthermore, in these areas management of freshwater resources, mostly stored in karst, coastal aquifers, is challenging if proper methods are not applied to detect possible critical situations of groundwater scarcity and deterioration.

In the area of the gulf of Taranto (southern Italy) these issues are particularly pressing, as the deep, karst aquifer is the only available source of freshwater and satisfies most of the human water-related activities. For these reasons, preserving this system through targeted management policies involves both natural and socio-economic aspects. A variable-density flow model was developed with SEAWAT to depict the "current" status of the saltwater intrusion within the aquifer. No appreciable effects were found to occur on the solution of the transport component due to different mathematical conceptualizations of the flow boundary conditions along the coast. Groundwater salinity stratification was found to occur, with salinity levels higher than a reference threshold within a strip spreading from 4 to 7 km from the coast in the deep aquifer. Such phenomenon would also affect some submarine freshwater springs, like the Citro Galeso.

A sensitivity analysis was used on two simulated scenarios with decreased rainfall and increased pumping. Differences in the concentration field with respect to the "current" status can be appreciated most in zones where the hydraulic conductivity of the deep aquifer is higher and the amount of these differences depends on flow boundary conditions. Furthermore, the presence of freshwater springs was found to influence the concentration field in different scenarios, causing an opposite behavior at shallow and higher depths.

Suggested Reviewers: Christian Langevin
U.S. Geological Survey
langevin@usgs.gov

He has a long experience on numerical tools for modeling groundwater-related processes.

Emilio Custodio
Dep. of Geotechnical Engineering and Geosciences, Technical University of Catalonia
emilio.custodio@upc.es

He has a long experience on groundwater studies in Mediterranean areas.

Philippe Renard
Centre d'hydrogéologie, Université des Neuchâtel
philippe.renard@unine.ch

He has a long experience on groundwater studies.

Jan Friesen
Department Catchment Hydrology, Helmholtz Centre for Environmental Research - UFZ
jan.friesen@ufz.de

He has a long experience on groundwater studies in semi-arid regions.

Leonor Rodriguez Sinobas
Universidad Politecnica de Madrid
leonor.rodriiguez.sinobas@upm.es
She has a long experience on groundwater studies for water management issues.

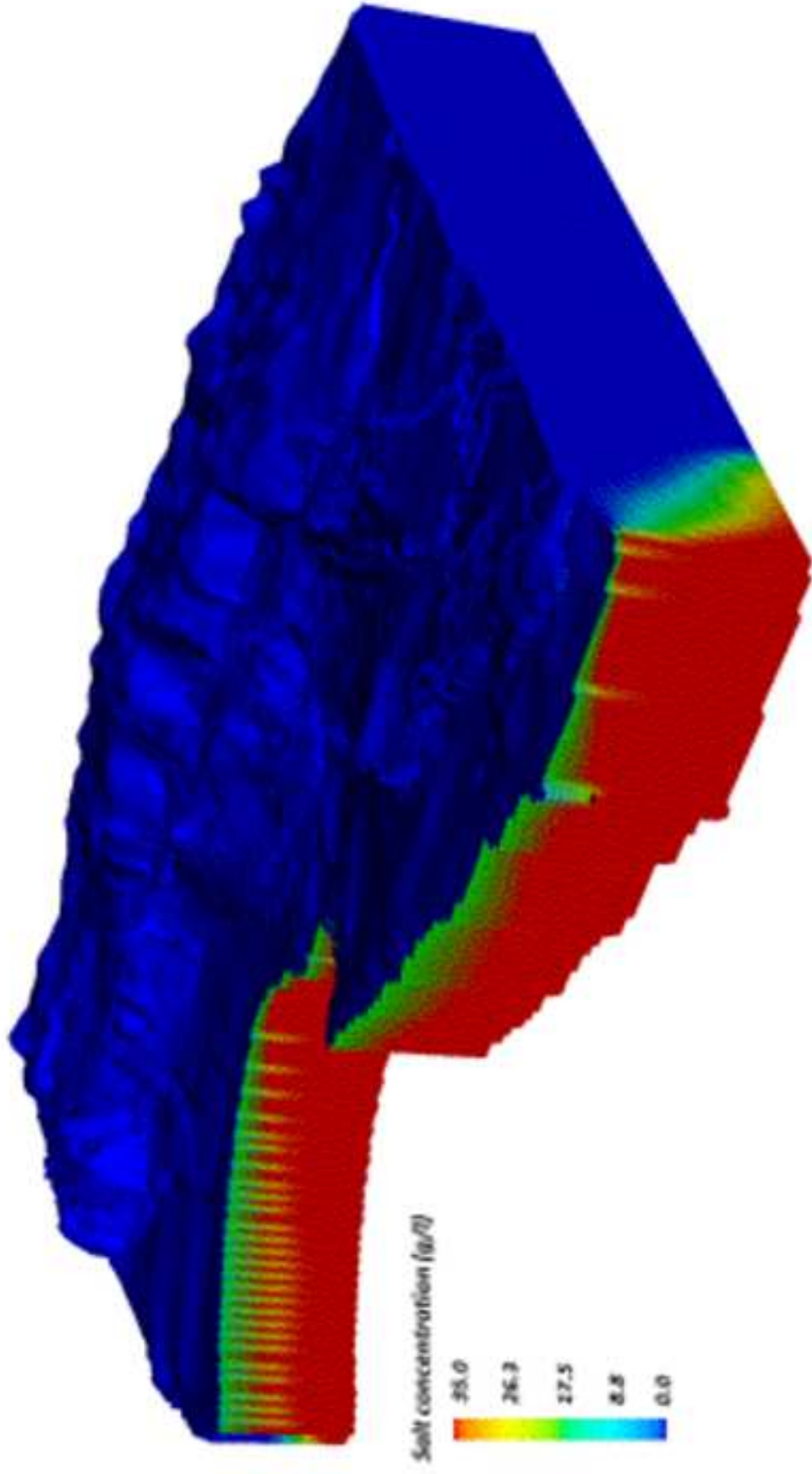
Opposed Reviewers:

*Cover Letter

1 This paper presents a solute transport model, which aims at assessing the occurrence of the saltwater
2 intrusion phenomenon in the karst, coastal aquifer of the Taranto area (southern Italy).

3 In the study area, this issue is particularly pressing, as the deep, karst aquifer is the only available
4 source of freshwater and satisfies most of the human water-related activities. For this reason,
5 preserving such system through targeted management policies involves both natural and socio-
6 economic aspects. In this framework, the scope of the analysis presented in this paper is to address
7 and support planning and management decisions, in order to prevent and restore critical situations,
8 with particular attention to groundwater quality of submarine freshwater springs.

9 A sensitivity analysis was further carried on to show the effects of different scenarios of natural
10 forcing and human interactions, i.e., decreasing rainfall recharge and increasing groundwater
11 abstraction, which are particularly severe in semi-arid, coastal areas where growing population
12 pressure might cause notable groundwater level declines and deterioration in water quality.



***Highlights (for review)**

- Assessing saltwater intrusion phenomenon in a karst, coastal aquifer for management issues
- Assessing groundwater quality of freshwater springs
- Testing the effects of different kinds of boundary conditions to model the groundwater flow component
- Testing the effects of different scenarios of natural forcing and human interactions

Seawater intrusion in karst, coastal aquifers: current challenges and future scenarios in the Taranto area (southern Italy)

Giovanna De Filippis^(1,2,3), Laura Foglia⁽⁴⁾, Mauro Giudici^(2,3,5), Steffen Mehl⁽⁶⁾, Stefano Margiotta^(7,8), Sergio Luigi Negri^(7,8)

1 – Land Lab, Dipartimento di Scienze della Vita, Scuola Superiore Sant’Anna (Pisa)

2 - Consorzio Interuniversitario per la Fisica delle Atmosfere e delle Idrosfere (CINFAI)

3 - Dipartimento di Scienze della Terra "A. Desio", Università degli Studi di Milano

4 - Institut für Angewandte Geowissenschaften, Technische Universität Darmstadt

5 - Istituto per la Dinamica dei Processi Ambientali (IDPA-CNR)

6 - Department of Civil Engineering, California State University, Chico, CA

7 - Laboratorio di Idrogeofisica e Stratigrafia per i Rischi Naturali, DISTeBa, Università del Salento

8 - Geomod srl, Spin-off of DISTeBA (Università del Salento)

Corresponding author: Giovanna De Filippis

Corresponding author’s e-mail: g.defilippis@sssup.it

Abstract

Arid and semi-arid regions in the Mediterranean area are characterized by very complex hydrogeological systems, about which limited knowledge is available due to the lack of data.

Furthermore, in these areas management of freshwater resources, mostly stored in karst, coastal aquifers, is challenging if proper methods are not applied to detect possible critical situations of groundwater scarcity and deterioration.

In the area of the gulf of Taranto (southern Italy) these issues are particularly pressing, as the deep, karst aquifer is the only available source of freshwater and satisfies most of the human water-related activities. For these reasons, preserving this system through targeted management policies involves both natural and socio-economic aspects.

A variable-density flow model was developed with SEAWAT to depict the “current” status of the saltwater intrusion within the aquifer. No appreciable effects were found to occur on the solution of the transport component due to different mathematical conceptualizations of the flow boundary

35 conditions along the coast. Groundwater salinity stratification was found to occur, with salinity levels
1
236 higher than a reference threshold within a strip spreading from 4 to 7 km from the coast in the deep
3
437 aquifer. Such phenomenon would also affect some submarine freshwater springs, like the Citro
6
738 Galeso.

8
9
1039 A sensitivity analysis was used on two simulated scenarios with decreased rainfall and increased
11
1240 pumping. Differences in the concentration field with respect to the “current” status can be
13
1441 appreciated most in zones where the hydraulic conductivity of the deep aquifer is higher and the
15
16
1742 amount of these differences depends on flow boundary conditions. Furthermore, the presence of
18
1943 freshwater springs was found to influence the concentration field in different scenarios, causing an
20
21
2244 opposite behavior at shallow and higher depths.

23
2445
25
26
2746 **Keywords:** saltwater intrusion, karst coastal aquifers, Mediterranean area, sensitivity analysis,
28
2947 groundwater management

30 3148 32 33 3449 **1. Introduction**

35
3650 Europe has a long coastline, both along the continent and islands, with areas that have been settled by
37
38
3951 humans since a long time ago. In the southern parts of Europe, especially along the Mediterranean
40
4152 shore, human water-related activities (e.g., irrigated agriculture and tourism) have largely increased
42
43
4453 freshwater demand in the 20th century; for instance, in southern Italy, about 45% of the total
45
4654 population is living in coastal areas settled since the mid-20th century (Custodio, 2010). In these areas
47
48
4955 available surface-water resources are often scarce or nonexistent making coastal aquifers important
50
5156 as they are often the only available freshwater resource for irrigation, tourism and other human
52
53
5457 activities. Subsequently, intensive exploitation of groundwater, and mismanagement have caused
55
5658 additional upset of the natural balance between surface water, groundwater, and seawater. This is
57
58
5959 particularly true for carbonate massifs, which are common along the European Mediterranean coast.
60
61
62
63
64
65

60 As a consequence, salinity problems in Mediterranean coastal areas have attracted the attention of
1
261 researchers, professionals, and specialists in recent decades.
3

4
562 Geochemical and geophysical surveys are often used to map and monitor saltwater intrusion in
6
763 coastal aquifers (see, e.g., Bouderbala, 2015 and references therein). Proper management of saltwater
8
9
1064 intrusion problems requires good knowledge of the aquifer system and the ability to forecast its
11
1265 future behavior under different scenarios of natural forcing and human interactions (Werner et al.,
13
14
1566 2012; Lambeck et al., 2011; Green and MacQuarrie, 2014; Okello et al., 2015). In this regard,
16
1767 numerical simulation is a commonly used tool to investigate saltwater intrusion in coastal aquifers
18
19
2068 and to assess alternative groundwater resource-management scenarios (Bear et al., 1999). Amongst
21
2269 available modeling approaches, variable-density groundwater flow models that track saltwater
23
2470 movement may be divided into interface models and dispersive solute-transport models (Bakker et
25
26
2771 al., 2013). In interface models, freshwater and seawater are separated by a sharp interface (see, e.g.,
28
2972 Bakker et al., 2013; De Filippis et al., 2015; Masciopinto, 2006; Mehdizadeh et al., 2015), while in
30
31
3273 dispersive solute-transport models (e.g., SUTRA, Voss and Provost, 2010; FEFLOW, Diersch, 2014;
33
3474 SEAWAT, Guo and Langevin, 2002), fluid density can vary continuously or from cell to cell in a
35
36
3775 model domain. Generally, a 3D saltwater intrusion model is not simple to apply due to the
38
3976 complexity of the involved physical processes and the basin geometry, the scarcity of adequate
40
4177 hydrogeological field data, and the heterogeneity of hydrogeological characteristics (Dentoni et al.,
42
43
4478 2015).

45
4679 This paper takes into account the implications on the groundwater quality and availability, related to
47
48
4980 the saltwater intrusion as a natural- and human-induced phenomenon. Here a large-scale variable-
50
5181 density flow model is proposed for the aquifer system of the province of Taranto with both technical-
52
53
5482 scientific and management-oriented aims. The numerical code SEAWAT was applied to develop a
55
5683 dispersive solute-transport model to assess the occurrence and extent of the saltwater intrusion in the
57
58
5984 aquifer of the Jonian coastal area of the Taranto province (southern Italy).
60
61
62
63
64
65

85 From a scientific point of view, the focus is on the sensitivity of model results to different boundary
1
286 conditions along the coast, which are not easy to determine due to the complex geological setting.
3
4
587 Such a complexity is very high in the most environmentally critical regions of Mar Piccolo and Mar
6
788 Grande, two shallow lagoon-like basins of fundamental importance for ecosystem and socio-
8
9
1089 economic contexts (mussels cultivation). In particular, the main objective is to improve the reliability
11
1290 of the estimated extent of saline intrusion both horizontally (inland) and vertically (among and inside
13
14
1591 individual hydrostratigraphic units). From a practical point of view, the model is also used to assess
16
1792 the possible effects that changes related to climate variability and human pressure have on these
18
19
2093 freshwater underground resources.
21
22
23

2495 2. Study area and objectives

26
2796 This study focuses on a coastal, multi-layered aquifer located in southern Italy. The study area
28
2997 (Figure 1) extends over about 2800 km² and includes most of the province of Taranto (40°25'05" N
30
31
3298 17°14'27" E), between the Murge plateau to the north and the Jonian coast to the south.
33
34
35

36
37
38
39100 **Figure 1.** Location of the study area. The color map refers to the Digital Terrain Model (DTM,
40
41
42101 horizontal spatial resolution of 500 m). The dashed areas delineate the contaminated Site of National
43
44102 Interest, as declared by the Italian Ministerial Decree dated September 20th 2001. Boundary
45
46
47103 conditions along the northern, western and eastern boundaries are highlighted (modified after De
48
49104 Filippis et al., 2015).
50

51
52
53
54105
55
56106 Within the study area, the zones near the city of Taranto have been the subject of interest for the
57
58
59107 scientific community in recent decades (see, e.g., Alabiso et al., 1997; Cardellicchio et al., 2007;
60
61108 Cavallo and Stabili, 2002; De Serio et al., 2007; Storelli and Marcotrigiano, 2000; Umgiesser et al.,
62
63
64109 2007; Zuffianò et al., 2015). As already assessed in previous studies (see, e.g., Giudici et al., 2012;
65
66110 De Filippis et al., 2013; De Filippis et al., 2015), the Taranto area is one of the most sensitive coastal

111 regions of southern Italy to seawater intrusion, because of the complex hydrostratigraphic
1
112 configuration and the presence of highly water-demanding human activities (e.g., industry,
3
113 agriculture). The presence of several kinds of polluting activities (i.e., commercial, shipping,
4
5
6
114 industrial and urban-related) occurring near Taranto is noteworthy and makes such area “at high risk
7
8
9
115 of environmental crisis” (Italian Ministerial Decree dated September 20th 2001, dashed areas in
10
11
116 Figure 1) and an ideal target for scientific research. One of the most critical areas of concern is the
13
14
117 highly vulnerable Mar Piccolo, which corresponds to a complex ecosystem, with strong interactions
15
16
118 among several environmental components, including groundwater due to the presence of relevant
17
18
19 submarine freshwater springs. For this reason, the study of this area was conducted with a
20
21
120 multidisciplinary approach by several research units within the Flagship Project RITMARE (the
22
23
121 Italian research for the sea).

24
25
26
122 In this paper, the relationship between groundwater and saltwater in the study area is analyzed with
27
28
123 particular attention to three main factors: 1) the occurrence of high-flux freshwater springs within the
29
30
124 Mar Piccolo seawater basin, 2) the presence of large fractures in karst formations, a characteristic
31
32
33
125 which is shared with most of the European Mediterranean coast, and 3) extensive withdrawals and/or
34
35
126 climate changes which contribute to modification of the equilibrium between fresh- and salt-water.
36
37
38

127 39 40 128 **3. Methods** 41 42

43
129 The aims highlighted in the previous section were achieved by developing a numerical model which
44
45
130 solves the coupled equations for groundwater flow and salt transport, by using a dispersive solute-
46
47
131 transport approach.
48
49

50
132 Among dispersive solute-transport models, some programs (e.g., SUTRA and FEFLOW) solve the
51
52
133 flow and transport equations simultaneously, while others (e.g., SEAWAT) have the option to solve
53
54
55
134 the transport equation separately using particle-based or finite-difference methods and compute a
56
57
135 new flow field to represent a changing density field. The latter approach and the SEAWAT
58
59
136 (Langevin et al., 2008) code are used in this paper.
60
61
62
63
64
65

137 3.1 Groundwater model setup

138 The geological, hydrodynamic and numerical features set to represent the aquifer system of the
139 Taranto area with respect to groundwater dynamics are described in De Filippis et al. (2015).

140 The multi-layered aquifer system is characterized by a heterogeneous hydrogeological structure,
141 which consists of the following hydrostratigraphic units (HUs):

- 142 • Cont&Terr HU, characterized by calcarenitic terraced deposits, covered by recent Continental
143 deposits with generally low permeability;
- 144 • SubCl HU, made of impermeable Subappennine clays;
- 145 • GCalc HU, characterized by coarse-grained Gravina calcarenites containing shallow aquifers
146 with limited extent;
- 147 • Gal HU, made of fine-grained and very compact limestones, marls and deposits of sandy
148 clays belonging to the Galatone formation;
- 149 • AltLim HU, mostly corresponding to the karst Altamura limestone and containing the deep
150 aquifer of the Salento peninsula. This HU is the most noteworthy, due to its karst features and
151 because the deep aquifer feeds the submarine springs in the Mar Piccolo. Furthermore, it is
152 the most susceptible to issues related to groundwater deficiency, due to climate changes and
153 exploitation for human water-related activities.

154 The study area (Figure 1) was discretized using square cells with 500 m side-length in the
155 horizontal plane. The vertical discretization extends from the ground surface, as determined by a
156 Digital Terrain Model (DTM - Figure 1) down to 500 m below the mean sea level (msl). Notice that
157 the ground surface varies in the study area from the sea level up to more than 500 m above msl in
158 the northern part of the domain. 14 layers with variable thicknesses have been introduced (Figure
159 2).

160 The uppermost four layers correspond, from top to bottom, to the Cont&Terr, SubCl, GCalc and
161 Gal HUs, while the AltLim HU was discretized in 10 layers (hereinafter referred to as AltLim
162 HU_1, AltLim HU_2 and so on, from top down). This choice is due to the variable thickness of the

AltLim HU in the study area, from about 300 m along the coastline to more than 1000 m inland, where this HU widely outcrops (see Figure 2). Moreover, the saltwater intrusion particularly affects the AltLim HU and the additional vertical discretization is needed to improve the representation of this phenomenon.

Figure 2. Vertical discretization of the aquifer system - (top) east side view; (bottom) west side view.

The four uppermost layers were considered homogeneous, with hydraulic conductivities set to 10^{-4} m/s for the Cont&Terr and GCalc HUs and 10^{-6} m/s for the SubCl and Gal HUs. Hydraulic heterogeneity of the AltLim HU was taken into account by estimating its conductivity through a direct calibration method as implemented in the Comparison Model Method (CMM) embedded within the YAGMod computer code, whose application to the same case study is presented in detail by De Filippis et al. (2015).

For the aims of this discussion, the hydraulic conductivity field shown in Figure 3 is used for the AltLim HU and the related model layers. This field was estimated based on the available head observations and defined source terms, as reported in De Filippis et al. (2015), and was obtained by applying a sharp interface approach (specifically the Ghyben-Herzberg approximation) for the calculation of the saturated thickness of the deep aquifer.

Figure 3. (a) Hydraulic conductivity field of the AltLim HU estimated with the Comparison Model Method (modified after De Filippis et al., 2015). (b) Locations of the salinity vertical profiles drawn in Figure 6 (symbols), of the profiles of the cross sections shown in Figure 7 (lines) and of the inner area mapped in Figures 5 and 8 (red rectangle).

188 The conductivity field obtained for the AltLim HU (Figure 3) shows a large spatial variability,
1 especially along the coastline, with values spanning over four orders of magnitude. The lowest
189 values (of the order of 10^{-4} m/s) were calculated inland and along the extremely western Jonian
3 values (of the order of 10^{-4} m/s) were calculated inland and along the extremely western Jonian
4 coast, while the highest ones (of the order of 10^{-1} m/s) were along the central and eastern coastline.
5
6
191 Aquifer recharge and groundwater extractions estimated by De Filippis et al. (2015) are used. In
8
9
192 In particular, about 37% of the total annual rainfall was estimated to infiltrate over the study area,
10
11
193 corresponding to a total inflow of almost $19 \text{ m}^3/\text{s}$. This areal recharge term was applied to the
13
14
194 uppermost active model layer. Furthermore, total extracted flow rates over the whole Province for
15
16
195 irrigation ($1.33 \text{ m}^3/\text{s}$), industrial ($0.86 \text{ m}^3/\text{s}$) and drinking ($0.25 \text{ m}^3/\text{s}$) purposes were distributed
17
18
196 according to different criteria (i.e., the land use map, the water need of different crops or the size of
19
20
197 industries). The estimated withdrawal terms were equally distributed among layers from AltLim
21
22
198 HU_1 to AltLim HU_10, as the deep aquifer is the most exploited at the large scale for human
23
24
199 water needs (i.e., irrigation, industry, drinking water). As a further extraction term, terrestrial and
25
26
200 submarine freshwater springs were simulated as discharging drains. Some of them, mostly located
27
28
201 in the plain north-west of Taranto, are fed by the shallow aquifer in the Cont&Terr HU, with mean
29
30
202 flow rates of the order of $0.1 \text{ m}^3/\text{s}$, except for the Tara spring, which is fed by the deep aquifer,
31
32
203 whose measured flow rate is more than $3 \text{ m}^3/\text{s}$, and which feeds the Ilva plant, the steelwork with
33
34
204 the highest output capacity in Europe. The springs located near Taranto are fed by the deep aquifer,
35
36
205 with highest flow rates up to $0.75 \text{ m}^3/\text{s}$ (see De Filippis et al., 2015 for details). For the development
37
38
206 of the numerical model, drains conductances were set as explained below.
39
40
41
42
207 No-flow boundaries were imposed along the left and right boundaries of the domain. An inflow of
43
44
208 about $1.13 \text{ m}^3/\text{s}$ was estimated to occur from the Murge plateau, by multiplying the mean annual
45
46
209 rainfall (about $600 \text{ mm}/\text{year}$) and the estimated recharge area identified by using measurements of
47
48
210 water level under static conditions (Regione Puglia, 2009) beyond the northern boundary of the
49
50
211 study area. This total inflow was simulated through recharge wells located within 75 cells in the
51
52
212 central part of the northern boundary, with equal flow rates equally distributed among model layers
53
54
213
55
56
57
58
59
60
61
62
63
64
65

214 AltLim HU_1 to AltLim HU_10 (as the AltLim HU outcrops in that zone). No flow was imposed at
1
215 the remaining cells of the same border (see Figure 1).
3
4
216 Boundary conditions along the coastline were conceptualized in two different ways to assess
5
6
217 possible effects on the simulation of the transport process. In the first configuration (hereinafter
7
8
218 referred to as gw_model1) Dirichlet boundary conditions were set along the coastline in all model
9
10
11
219 layers with head values equal to the msl (hydraulic contact is assumed to occur at the coast). In the
12
13
220 second configuration (hereinafter referred to as gw_model2) the same Dirichlet boundary
14
15
16
221 conditions were set along the coastline in model layers Cont&Terr and SubCl HUs, while no-flow
17
18
222 boundary conditions were applied to the underlying layers, due to the presence of a normal fault in
19
20
21
223 the zone of the submarine springs within the Mar Piccolo, which could halt groundwater flow in the
22
23
224 AltLim HU, at least at shallow depths, because a direct contact between such HU and the poorly
24
25
225 permeable Subappennine clays would occur (Figure 4). With respect to what was done in De
26
27
226 Filippis et al. (2015), here drain conductances were further decreased by $\frac{1}{4}$ to avoid negative
28
29
227 hydraulic heads (i.e., below the msl) at some locations due to particular boundary conditions in
30
31
32
228 gw_model1.
33
34
35
36
37
38

229
39
40
41
42
43
44
45
46
47
48
49
50
51
52
53
54
55
56
57
58
59
60
61
62
63
64
65

Figure 4. Schematic hydrogeological sketch nearby the Galeso spring (modified after Margiotta et al., 2010).

233 The groundwater flow model was run over six months at steady-state using three stress periods with
234 time steps of two months. As mentioned in Guo and Langevin (2002), there is no option to run the
235 transport model as steady-state in SEAWAT, so the transport component is run in transient
236 conditions, even if the flow is specified as steady-state.

237 To reduce the model complexity and avoid many dry cells and numerical difficulties, the simulation
238 was run with all layers under confined conditions. An unconfined simulation was performed to
239 check the mass balance terms and showed good agreement between the confined and unconfined

240 models. For example, the difference between the net aquifer balance simulated under confined and
1
241 unconfined conditions is of the order of 10^{-5} m³/s for gw_model1 and 10^{-6} m³/s for gw_model2.
3
4

242 3.2 Transport model setup 5 6

243 In this work, an implicit finite-difference scheme is used, so that the flow and transport equations are
7
1244 repeatedly solved several times within the same time step until the maximum difference in fluid
11
1245 density between consecutive iterations is less than a user-specified tolerance, set to 10^{-6} kg/m³.
12
13
14

1246 The molecular diffusion coefficient was set to 10^{-6} m²/s for each model layer: the longitudinal
15
16
17
1247 dispersivity (α_L) was assigned a value of 50 m, i.e., one tenth of the spatial horizontal discretization
18
19
2048 (Gelhar et al., 1992), the ratios between α_L and the horizontal and vertical transverse dispersivities
21
22
249 were assigned the values of 0.1 and 0.01, respectively (Zheng and Wang, 1999).
23
24

250 Furthermore, both the advection and dispersion terms of the transport equation contain the effective
25
26
27
251 porosity of the medium. Here the following values were assumed: 0.3 for Cont&Terr and GCalc
28
29
3042 HU, 0.5 for SubCl and Gal HUs and 0.1 for the AltLim HU.
31

3253 To calculate the sink/source terms, concentration must be defined for each sink/source of the
32
33
34
354 groundwater model. Zero concentration was specified for the recharge from rainfall (i.e., Dirichlet
35
36
3755 transport boundary condition), while in the remaining sinks/sources cells concentration could vary
38
39
256 freely, according to what was calculated through the transport equation.
40
41

4257 Dirichlet transport boundary conditions were defined along the coastline for all layers by specifying a
42
43
44
258 concentration of 35 g/L to represent seawater.
45
46

4259 Both groundwater and transport models share the same time-discretization scheme, but the transport
47
48
4960 equation is solved under transient conditions and repeatedly within a time-step, as the transport
49
50
51
261 solution has either stability constraints and/or accuracy requirements that are more restrictive than
52
53
54
262 those for the flow solution. Each time-step is further divided into smaller transport-steps, during
54
55
56
263 which heads are constant.
56
57
58

264 265 4. Results and scenarios 60 61 62 63 64 65

266 The two models developed with two different configurations of the flow component (gw_model1 and
1
267 gw_model2) were used to test possible effects of flow boundary conditions on the transport model
3
4
268 solution. In this regard, no remarkable differences were found in the simulated concentration field.
5
6
269 As an example, in Figure 5 the 0.5 g/L salinity contour lines are drawn for both configurations (red
7
8
270 line for gw_model1 and black line for gw_model2) and for different model layers in the inner zone
9
10
11
1271 shown in Figure 3.
13

14
15
16
1273 **Figure 5.** Contour lines for a salinity of 0.5 g/L simulated with configurations set in gw_model1 (red
17
18
19
20
274 lines) and gw_model2 (black lines), for the following model layers: (a) GCalc HU, (b) AltLim HU_1,
21
2275 (c) AltLim HU_5, (d) AltLim HU_10. Zoom of the inner area bounded in Figure 3.
23

24
25
26
277 Considering the contour line of 0.5 g/L as a reference threshold for salinity in groundwater
27
28
278 (Cotecchia et al., 2005), we can assess that the saltwater intrusion phenomenon should affect also
29
30
31
3279 porous aquifers hosted in the GCalc HU. Focusing on the deep aquifer hosted in the AltLim HU, we
32
33
34
35
36
37
281 can infer that the spreading of intrusion gradually advances towards inland, from about 4 km from the
38
39
40
41
42
43
44
45
46
47
48
49
50
51
52
53
54
55
56
57
58
59
60
61
62
63
64
65

282 Figure 6 shows three salinity vertical profiles at three different locations near the coast, while Figure
283 7 shows two 2D sections, where the locations of some drains are highlighted.

284
285 **Figure 6.** Salinity profiles along vertical grid columns at locations 1, 2 and 3 shown in Figure 3.
286 Values simulated with the gw_model2 configuration.

287
288 **Figure 7.** 2D sections along the profiles drawn in Figure 3 (20-fold vertical exaggeration): (top) WE
289 section; (bottom) SW-NE section. Values simulated with the gw_model2 configuration.

291 The salinity profiles shown in Figure 6 refer to locations inside the industrial and military area
1
292 (Location 1), near the Tara terrestrial spring (Location 2) and in correspondence of the Citro Galeso
3
4
293 submarine spring (Location 3). According to these profiles, there is an intense salinity stratification,
6
294 with lower values in the upper model layers (from Cont&Terr HU to Gal HU) and concentration
8
295 increasing gradually from AltLim HU_1 to AltLim HU_10. This conclusion is in accordance with
10
11
1296 previous works (see, e.g., Cotecchia et al., 2005 and references therein).
13

14
297 The cross sections shown in Figure 7 can help to estimate the extent of the saline plume through the
15
16
1298 model layers and with respect to the coastline. The locations of some submarine springs located
18
19
299 within the Mar Piccolo are also highlighted, to draw conclusions about the quality of the outflowing
20
21
300 freshwater. In this regard, the salt concentration simulated by the model at the elevation of the Galeso
22
23
301 spring is about 1.2 g/L, which is within the interval reported in Umgiesser et al. (2007). As a further
25
26
302 check, also the fraction of seawater was calculated at the elevation of the Galeso spring itself, as
27
28
303 defined in Zuffianò et al. (2015), i.e., the relative concentration of chloride ions (mol/L) with respect
30
31
304 to that of freshwater and saltwater. A value of 3.4% was obtained which, considering the model scale
32
33
305 used in the analysis presented here, is in good agreement with 5% calculated in Zuffianò et al.
35
36
306 (2015), based on field measurements and laboratory analysis.
37

38
307 Finally, a sensitivity analysis was performed to assess the effects of changing stresses on the model
40
41
308 budgets. In particular, two scenarios were defined, decreasing rainfall recharge by 10% and
42
43
309 increasing irrigation withdrawals by 25%, according to forecasts of the European Environment
44
45
310 Agency (EEA) for the 21st century. Hereinafter the “current” scenario will be referred as
47
48
311 “undisturbed conditions”, while the other two scenarios will be identified as “decreased recharge”
49
50
312 and “increased pumping”.

51
52
313 Differences in the simulated concentration fields are difficult to show with color maps, therefore in
54
55
314 Figure 8 the contour lines corresponding to a concentration of 10 g/L and 30 g/L are drawn for
57
58
315 AltLimHU_1 and AltLim HU_7, respectively, for both gw_model1 and gw_model2, to show the
59
60
316 effects of decreased recharge and increased pumping. The main differences in the simulated
62
63
64
65

317 concentration can be observed in areas where the hydraulic conductivity of the AltLim HUs (see
1
318 Figure 3) is higher, as here more recirculation can occur. Moreover, such differences are more
3
4
319 evident for gw_model1 due to the particular flow boundary condition which further enhances this
6
320 mechanism.

321
10
11
322 **Figure 8.** Salinity contour lines simulated for the three different scenarios: (a) 10 g/L for AltLim
13
14
323 HU_1 and gw_model1; (b) 30 g/L for AltLim HU_7 and gw_model1; (c) 10 g/L for AltLim HU_1
15
16
324 and gw_model2; (d) 30 g/L for AltLim HU_7 and gw_model2. Zoom over the area bounded in
18
19
325 Figure 3.

21
22
23
24
327 The salinity profiles shown in Figure 9 are evaluated at location 1 and refer to the three different
25
26
328 scenarios.

28
29
30
31
32
330 **Figure 9.** Salinity profiles along vertical grid columns at location 1 shown in Figure 3. Values
33
34
35
36
37
38
39
40
41
42
43
44
45
46
47
48
49
50
51
52
53
54
55
56
57
58
59
60
61
62
63
64
65

331 simulated with gw_model1 and gw_model2 configurations for the three different scenarios.
332
333 Figure 9 clearly shows that the effects of decreasing recharge and increasing pumping is reverse
334 above and below a certain depth around 200 m below the msl. In fact, from the uppermost layer to
335 the AltLim HU_7 (in gw_model1) or AltLim HU_8 (in gw_model2), the salinity levels simulated
336 after decreasing recharge and increasing pumping are lower than those estimated under undisturbed
337 condition. The major differences can be found within the AltLim HU_1 layer, probably due to the
338 presence of drains, whose flow rates are lower due to a decrease in the hydraulic head. As an
339 example, the salt concentration calculated in gw_model2 for the two scenarios is about 0.9 g/L at the
340 location of the Citro Galeso spring, with respect to 1.2 g/L simulated under undisturbed conditions.
341 At greater depths decreasing recharge or increasing pumping cause the concentration values to
342 increase and, as stated before, differences with respect to the undisturbed conditions are more

343 appreciable in gw_model1. Furthermore, the effects of decreased recharge and increased pumping are
1
344 reverse according to depth and flow boundary conditions: in gw_model1, higher concentration values
3
345 are simulated with decreased recharge at shallow depths and with increased pumping in the deepest
4
6 layers and vice versa for gw_model2. This is mostly due to the effects of different boundary
8
347 conditions on the increased pumping scenario: concentration values simulated with decreased
9
10 recharge (see red profiles in Figure 9), indeed, do not show appreciable differences between
11
1348 gw_model1 and gw_model2, while remarkable differences arise for the increased pumping scenario.
13
14
15349 This is reasonable, as increased pumping has greater effects than decreased recharge on the simulated
16
1350 processes in the deep aquifer (AltLim HU_1 through AltLim HU_10), considering that rainfall
18
1351 infiltration occurs through a thick (about 100 m) impermeable layer (SubCl HU).
20
21
22352

26 354 5. Conclusions

28
2355 The recurrence of drought years, groundwater over-exploitation and the rise of water demand
30
31
32356 associated with growing population along the coasts might cause notable groundwater level declines
33
357 and deterioration in water quality. In such areas, seawater intrusion has consequently occurred and
35
36
358 advanced inland causing salinity problems. This represents a threat to agriculture and water resources
37
38
359 as the coastal population mostly depends on groundwater for domestic use and irrigation. Therefore,
40
41
360 management of water resources in the coastal aquifers of arid areas, like southern Italy, requires
42
43
361 particular attention and sustainable management of groundwater is of paramount importance.
44

45
362 In this paper, the extent of the saltwater intrusion phenomenon was evaluated, especially focusing on
47
48
363 the deep, karst aquifer of the Taranto area, which satisfies the main socio-economic activities (e.g.,
49
50
364 agriculture and industry) and feeds the most important freshwater springs of the Apulia region.

52
53
365 According to the developed variable-density flow model, a wide strip along the coast in the deep
54
55
366 aquifer has salt concentration levels higher than the 0.5 g/L reference threshold. This strip spreads
57
58
367 from about 4 km to about 7 km from the coast with increasing depth. Moreover, this model confirms
59
60
61
62
63
64
65

368 the salinity stratification identified in some logs reported in the literature, as well as the fraction of
1
369 seawater calculated for the Citro Galeso spring.
3

370 The model was run considering two different kinds of boundary conditions along the coast for the
4
6
371 flow component, but had no remarkable effects on the transport solution.
8

372 A sensitivity analysis showed the effects of two possible future scenarios, representing respectively
9
10
11
12
13
14
15
16
17
18
19
20
21
22
23
24
25
26
27
28
29
30
31
32
33
34
35
36
37
38
39
40
41
42
43
44
45
46
47
48
49
50
51
52
53
54
55
56
57
58
59
60
61
62
63
64
65

373 decreased recharge and increased pumping on the salt concentration field. Differences were found to
374 be larger when using Dirichlet boundary conditions along the coast for the flow model and more
375 significant in areas where the hydraulic conductivity of the deep aquifer is higher. Furthermore, the
376 aquifer system was found to be negatively affected by these scenarios at great depths, i.e., higher
377 salinity levels were simulated with decreased recharge and increased pumping below about 200 m
378 depth with respect to the mean sea level, while the opposite was found at shallow depths. As an
379 example, the salt concentration at the location of the Citro Galeso spring would be lower under
380 perturbed conditions, so making “current” salinity values higher than those simulated with decreased
381 recharge and increased pumping. Moreover, major differences with respect to undisturbed conditions
382 were highlighted for the increased pumping scenario, which affects the deep aquifer much more than
383 what decreased recharge does.

385 **Acknowledgements**

386 The activities described in this paper were funded by the Flagship Project RITMARE - La Ricerca
387 Italiana per il Mare - coordinated by the National Research Council and funded by the Ministry for
388 Education, University and Research within the National Research Program 2011-2013.

390 **References**

391 Alabiso G, Cannalire M, Ghionda D, Milillo M, Leone G, Caciorgna O. Particulate matter and
392 chemical-physical conditions of an inner sea: the Mar Piccolo in Taranto. A new statistical approach.
393 *Marine Chemistry* 1997, 58:373-388.

- 394 Bakker M, Schaars F, Hughes JD, Langevin CD, Dausman AM. Documentation of the Seawater
1
395 Intrusion (SWI2) Package for MODFLOW. U.S. Geological Survey, Reston, Virginia; 2013.
3
4
5
396 Bear J, Cheng AHD, Sorek S, Ouazar D, Herrera I. Seawater intrusion in coastal aquifers: concepts,
6
7
397 methods, and practices. Kluwer, Dordrecht, The Netherlands; 1999.
9
10
1398 Bouderbala A. Groundwater salinization in semi-arid zones: an example from Nador plain (Tipaza,
12
13
399 Algeria). *Environ Earth Sci* 2015; 73:5479–5496. doi:10.1007/s12665-014-3801-9.
14
15
400 Cardellicchio N, Buccolieri A, Giandomenico S, Lopez L, Pizzulli F, Spada L. Organic pollutants
17
18
401 (PAHs, PCBs) in sediments from the Mar Piccolo in Taranto (Ionian Sea, Southern Italy). *Mar Pollut*
20
21
402 *Bull* 2007; 55:451-458. doi:10.1016/j.marpolbul.2007.09.007.
22
23
24
403 Cavallo RA, Stabili L. Presence of vibrios in seawater and *Mytilus galloprovincialis* (Lam.) from the
25
26
404 Mar Piccolo of Taranto (Ionian Sea). *Water Research* 2002, 36:3719-3726.
28
29
30
405 Cotecchia V, Grassi D, Polemio M. Carbonate Aquifers in Apulia and Seawater Intrusion. *Giornale*
31
32
406 *di Geologia Applicata* 2005; 1:219–231. doi:10.1474/GGA.2005-01.0-22.0022.
33
34
35
407 Custodio E. Coastal aquifers of Europe: an overview. *Hydrogeology Journal* 2010; 18:269-280. doi:
36
37
408 10.1007/s10040-009-0496-1.
39
40
41
409 De Filippis G, Giudici M, Margiotta S, Mazzone F, Negri S, Vassena C. Numerical modeling of the
42
43
410 groundwater flow in the fractured and karst aquifer of the Salento peninsula (Southern Italy). *Acque*
45
46
411 *Sotteranee* 2013; 2:17-28. doi:10.7343/AS-016-013-0040.
47
48
49
412 De Filippis G, Giudici M, Margiotta S, Negri SL. Conceptualization and characterization of a coastal
50
51
413 multi-layered aquifer system in the Taranto Gulf (southern Italy). *Environ Earth Sci* 2015 (accepted;
52
53
414 first minor revision completed).
55
56
57
415 De Serio F, Malcangio D, Mossa M. Circulation in a Southern Italy coastal basin: Modelling and
58
59
416 field measurements. *Continental Shelf Research* 2007, 27,6:779-797. doi:10.1016/j.csr.2006.11.018.
61
62
63
64
65

417 Dentoni M, Deidda R, Paniconi C, Qahman K, Lecca G. A simulation/optimization study to assess
1
418 seawater intrusion management strategies for the Gaza Strip coastal aquifer (Palestine).
2
3
4
419 Hydrogeology Journal 2015; 23:249–264. doi:10.1007/s10040-014-1214-1.
5
6
7
420 Diersch, H-J G. FEFLOW – Finite element modeling of flow, mass and heat transport in porous and
8
9
10 fractured media. Springer 2014; 996 pp. ISBN 978-3-642-38738-8, doi:10.1007/978-3-642-38739-5.
11
12
13
422 EEA (European Environment Agency). <http://www.eea.europa.eu/it>
14
15
16
423 Gelhar LW, Welty C, Rehfeldt KR. A critical review of data of field-scale dispersion in aquifers.
17
18
19
424 Water Resources Research 1992; 28:1955-1974.
20
21
22
425 Giudici M, Margiotta S, Mazzone F, Negri S, Vassena C. Modelling hydrostratigraphy and
23
24
426 groundwater flow of a fractured and karst aquifer in a Mediterranean basin (Salento peninsula,
25
26
427 southeastern Italy). Environ Earth Sci 2012. doi:10.1007/s12665-012-1631-1.
28
29
30
428 Green NR, MacQuarrie KTB. An evaluation of the relative importance of the effects of climate
31
32
429 change and groundwater extraction on seawater intrusion in coastal aquifers in Atlantic Canada.
33
34
430 Hydrogeology Journal 2014; 22:609–623. doi:10.1007/s10040-013-1092-y.
35
36
37
431 Guo W, Langevin CD. User's guide to SEAWAT: a computer program for simulation of three-
38
39
40 dimensional variable-density ground-water flow. U.S. Geological Survey, Tallahassee, Florida; 2002.
41
42
43
433 Lambeck K, Antonioli F, Anzidei M, Ferranti L, Leoni G, Scicchitano G, Silenzi S. Sea level change
44
45
434 along the Italian coast during the Holocene and projections for the future. Quaternary International
46
47
48
435 2011; 232:250-257. doi:10.1016/j.quaint.2010.04.026.
49
50
51
436 Langevin CD, Thorne DT, Dausman AM, Sukop MC, Guo W. SEAWAT Version 4: A Computer
52
53
437 Program for Simulation of Multi-Species Solute and Heat Transport. U.S. Geological Survey, Reston,
54
55
56
438 Virginia; 2008.
57
58
59
60
61
62
63
64
65

- 439 Margiotta S, Mazzone F, Negri S. Stratigraphic revision of Brindisi-Taranto plain: hydrogeological
1
2
3
4
5
441 Masciopinto C. Simulation of coastal groundwater remediation: the case of Nardo' fractured aquifer
6
7
442 in Southern Italy. Environmental Modelling & Software 2006; 21:85–97.
8
9
10
443 doi:10.1016/j.envsoft.2004.09.028.
11
12
13
444 Mehdizadeh SS, Vafaie F, Abolghasemi H. Assessment of sharp-interface approach for saltwater
14
15
445 intrusion prediction in an unconfined coastal aquifer exposed to pumping. Environ Earth Sci 2015;
16
17
446 73:8345–8355. doi:10.1007/s12665-014-3996-9.
18
19
20
21
447 Okello C, Antonellini M, Greggio N, Wambiji N. Freshwater resource characterization and
22
23
448 vulnerability to climate change of the Shela aquifer in Lamu, Kenya. Environ Earth Sci 2015;
24
25
449 73:3801–3817. doi:10.1007/s12665-014-3665-z.
26
27
28
29
450 Regione Puglia. Piano di Tutela delle Acque - Att.6.1 "*Archivio anagrafico ed analisi dei punti*
30
31
451 *acqua censiti (pozzi e sorgenti)*" – "*Data archive and analysis of groundwater surveys*". Compiled
32
33
452 by SOGESID S.p.A.; language: Italian; 2009.
34
35
36
37
453 Storelli MM, Marcotrigiano GO. Polycyclic aromatic hydrocarbon distributions in sediments from
38
39
454 the Mar Piccolo, Ionian Sea, Italy. Bull. Environ. Contam. Toxicol. 2000, 65:537-544.
40
41
455 doi:10.1007/s001280000157.
42
43
44
45
456 Umgiesser G, Scroccaro I, Alabiso G. Mass exchange mechanism in the Taranto Sea. Transitional
46
47
457 Waters Bulletin 2007, 2:59-71. doi:10.1285/i1825229Xv1n2p59.
48
49
50
458 Voss CI, Provost AM. SUTRA: A Model for Saturated-Unsaturated Variable-Density Ground-Water
51
52
459 Flow with Solute or Energy Transport. U.S. Geological Survey, Reston, Virginia; 2010.
53
54
55
56
460 Werner AD, Bakker M, Post VEA, Vandenbohede A, Lu C, Ataie-Ashtiani B, Simmons CT, Barry
57
58
461 DA. Seawater intrusion processes, investigation and management: recent advances and future
59
60
462 challenges. Adv Water Resour 2012; 51:3–26. doi:10.1016/j.advwatres.2012.03.004.
61
62
63
64
65

463 Zheng C, Wang PP. MT3DMS - A modular three-dimensional multispecies transport model for
1
464 simulation of advection, dispersion and chemical reactions of contaminants in groundwater systems.
3
4
465 The Hydrogeology Group, The University of Alabama; 1999.
6
7
466 Zuffianò LE, Basso A, Casarano D, Dragone V, Limoni PP, Romanazzi A, Santaloia F, PolemioM.
9
10
467 Coastal hydrogeological system of Mar Piccolo (Taranto, Italy). Environ Sci Pollut Res 2015.
11
12
468 doi:10.1007/s11356-015-4932-6.
13
14

469

16

17

470

18

19

20

21

22

23

24

25

26

27

28

29

30

31

32

33

34

35

36

37

38

39

40

41

42

43

44

45

46

47

48

49

50

51

52

53

54

55

56

57

58

59

60

61

62

63

64

65

Figure2
[Click here to download high resolution image](#)

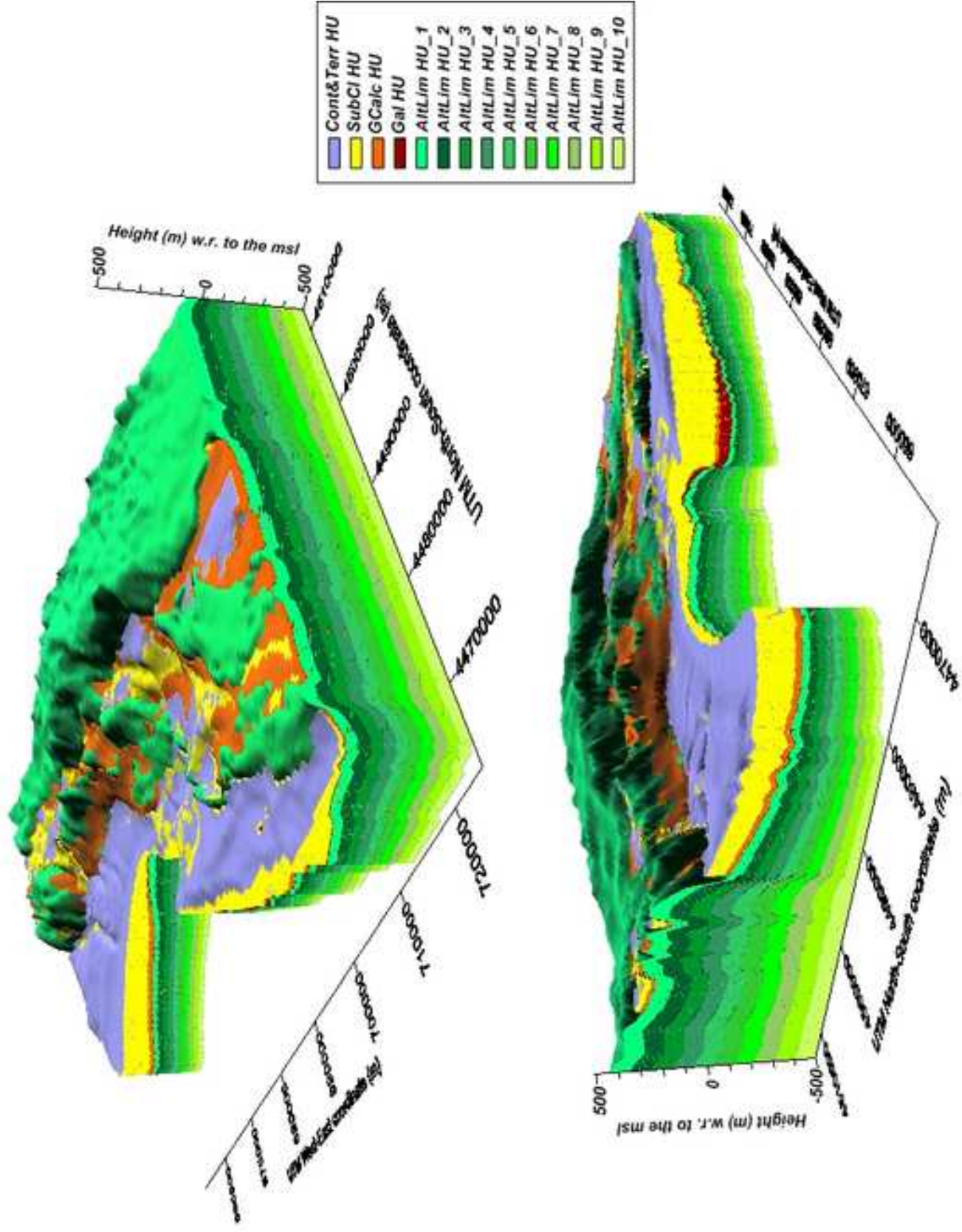
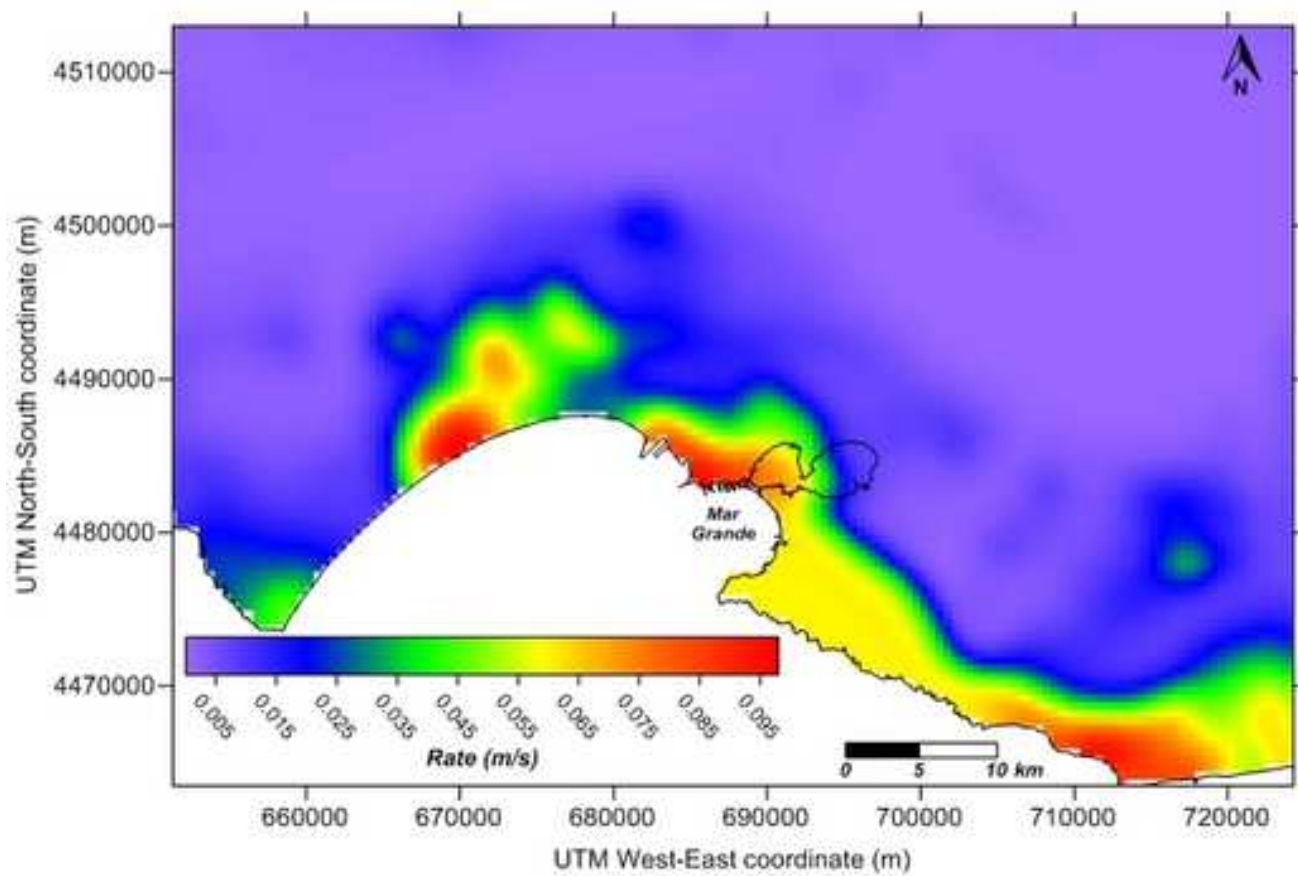
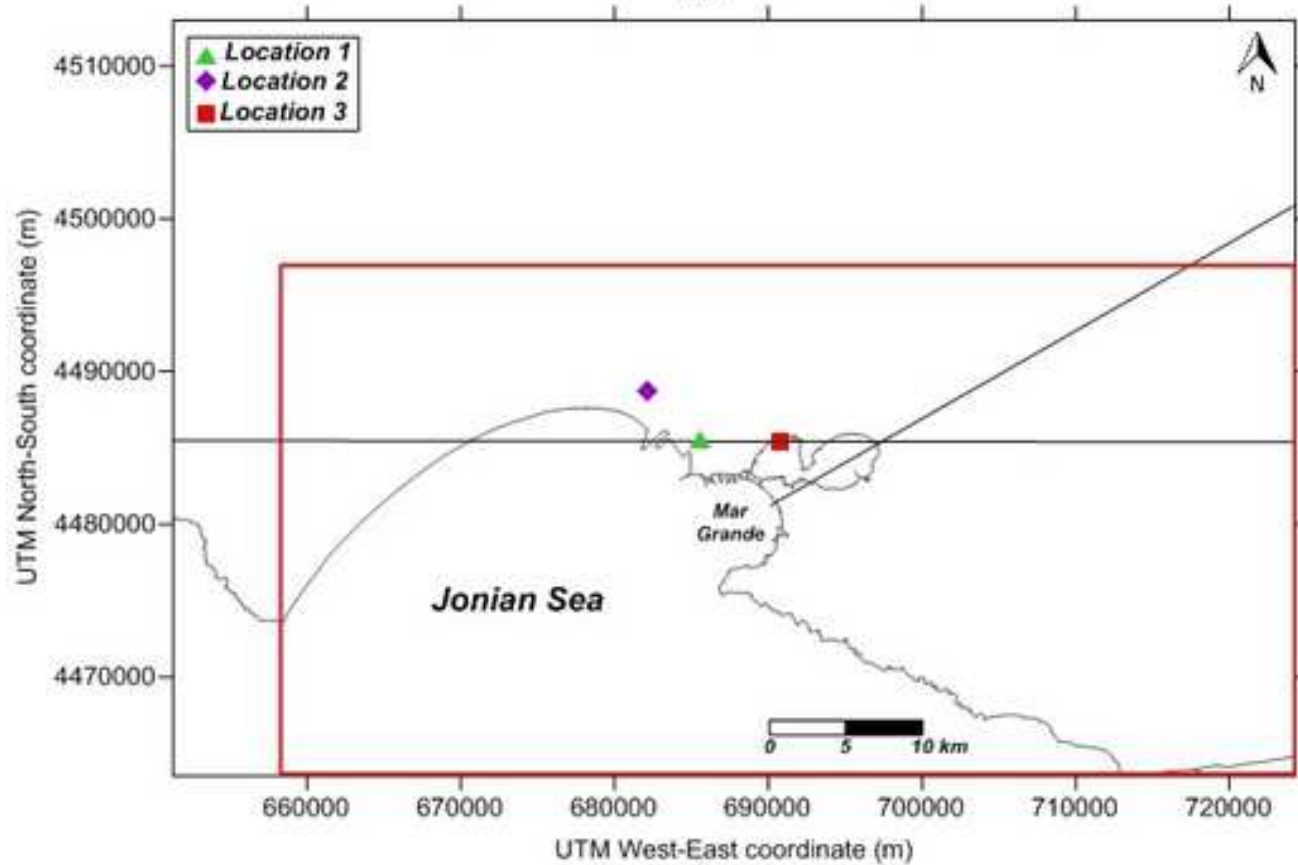


Figure3
[Click here to download high resolution image](#)



(a)



(b)

Figure4
[Click here to download high resolution image](#)

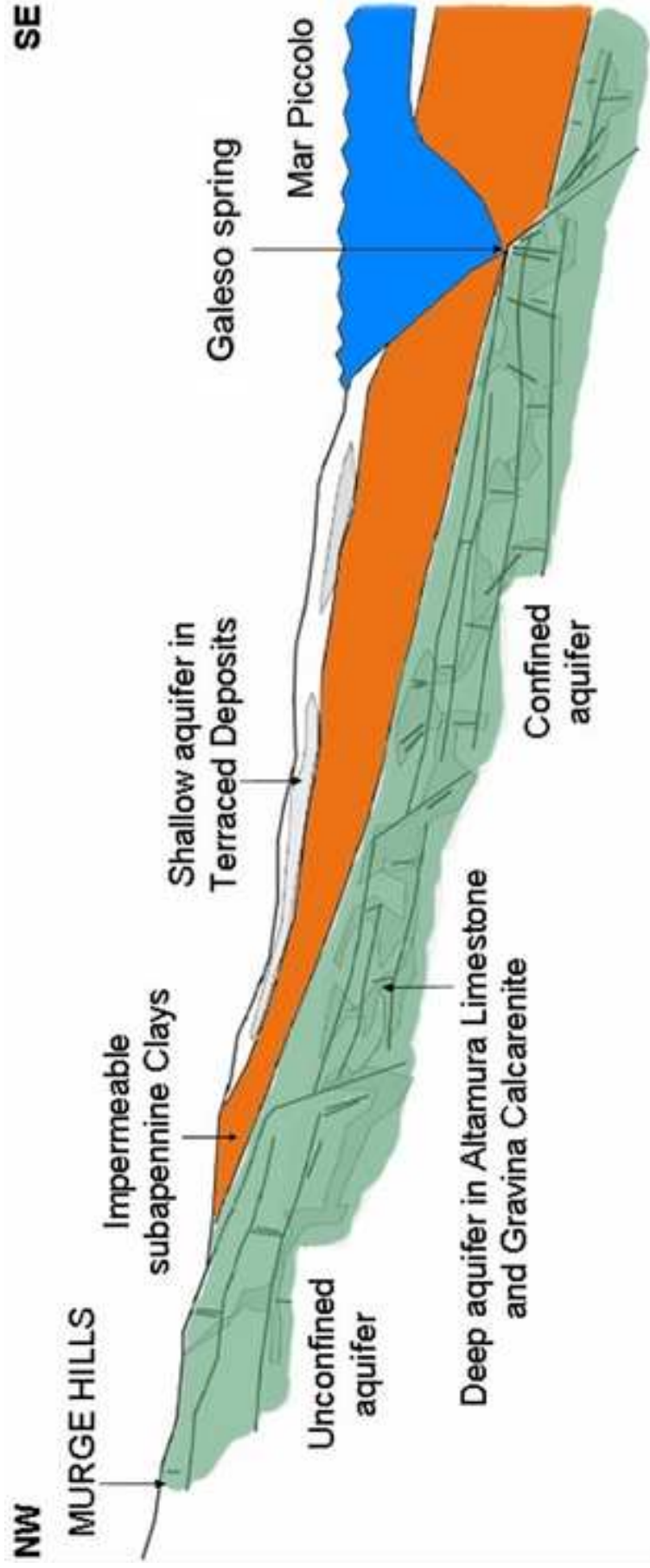


Figure5
[Click here to download high resolution image](#)

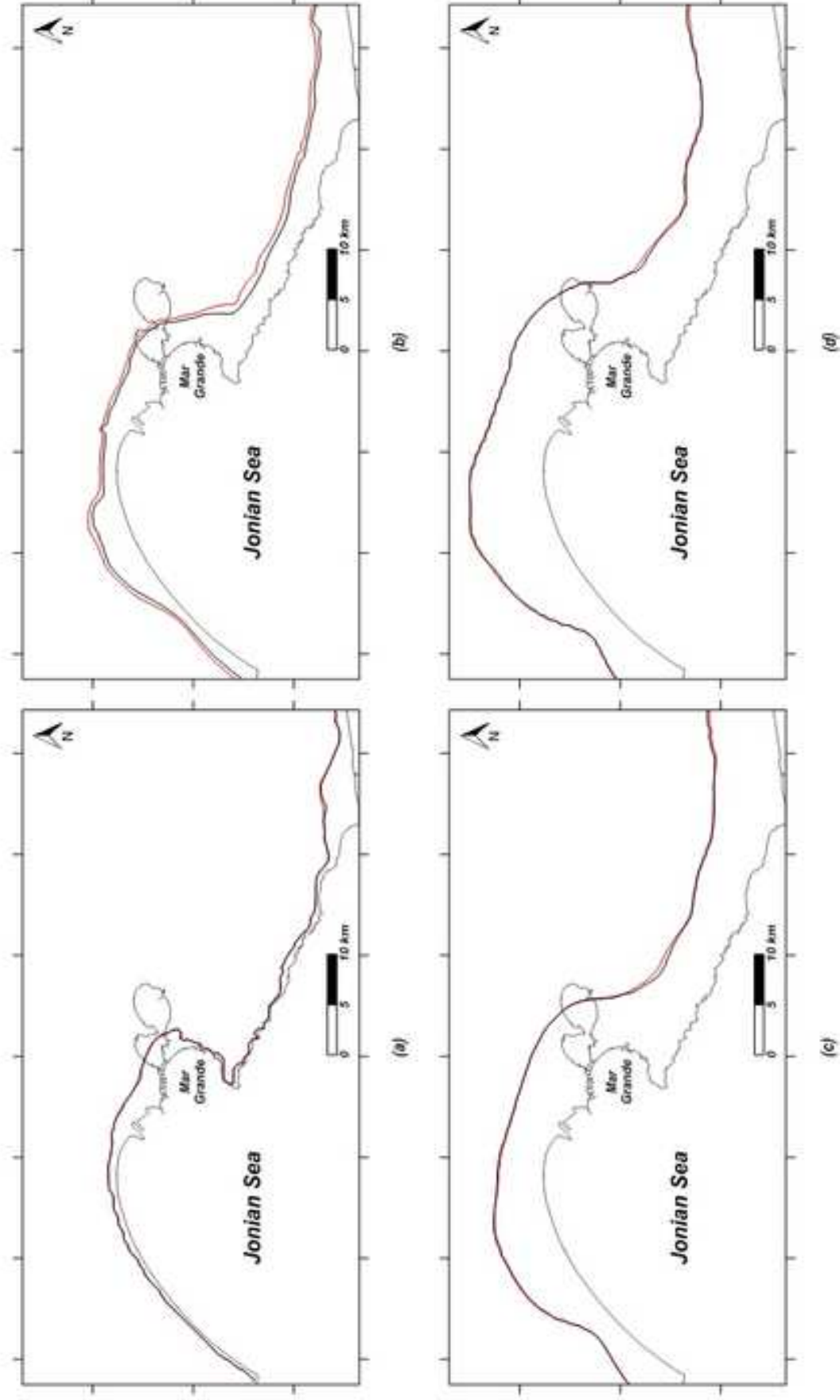


Figure6
[Click here to download high resolution image](#)

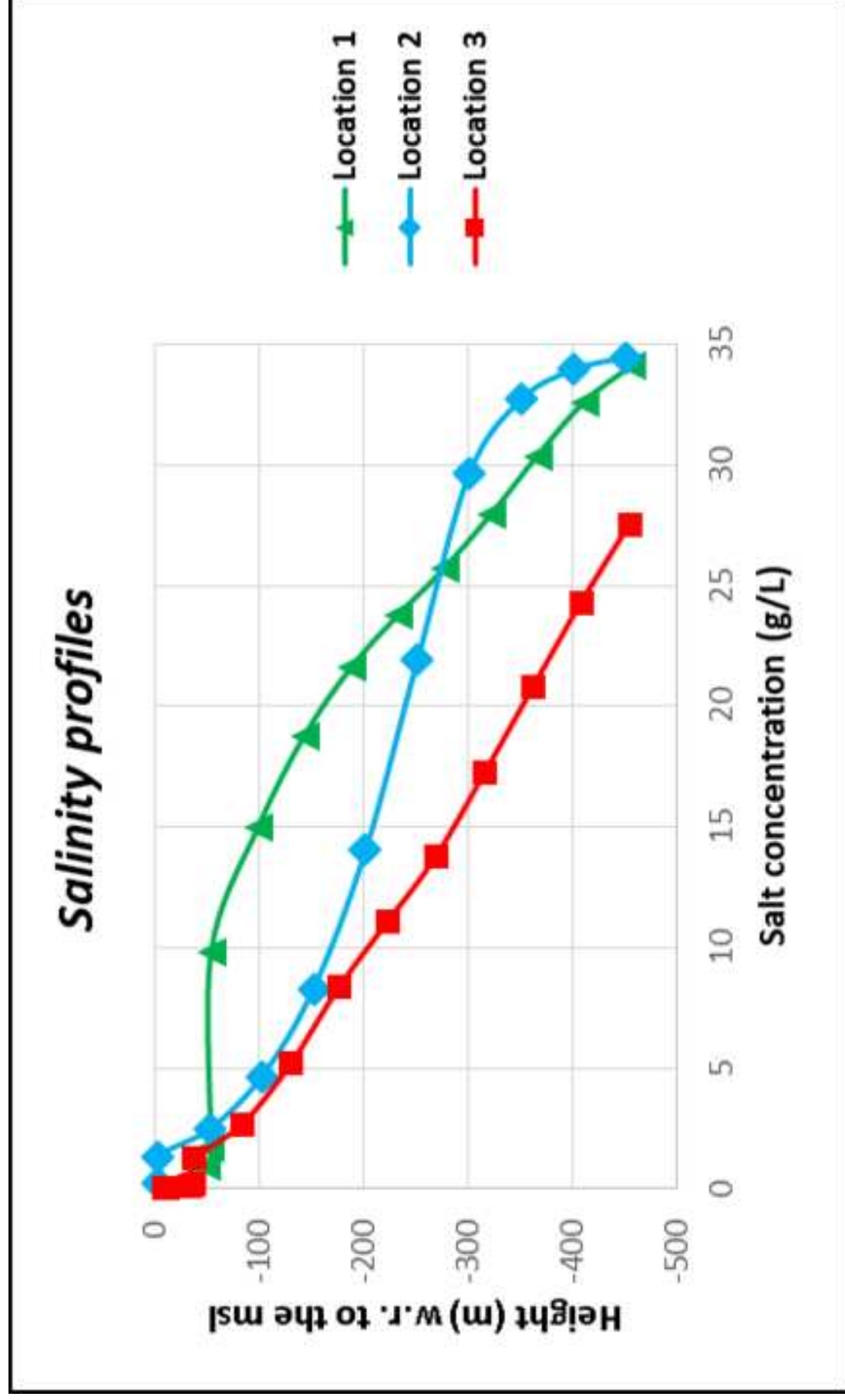


Figure7
[Click here to download high resolution image](#)

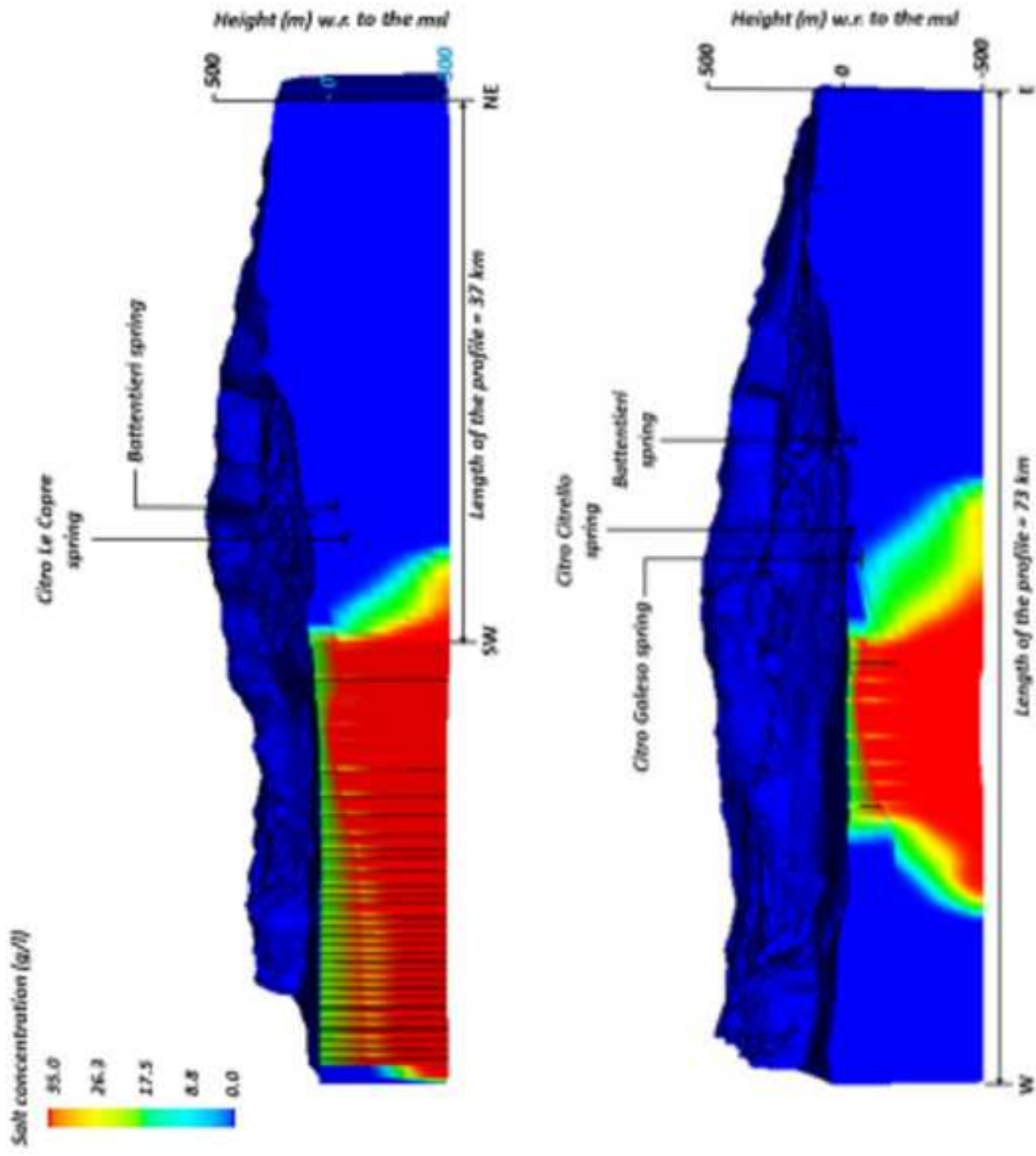


Figure8
[Click here to download high resolution image](#)

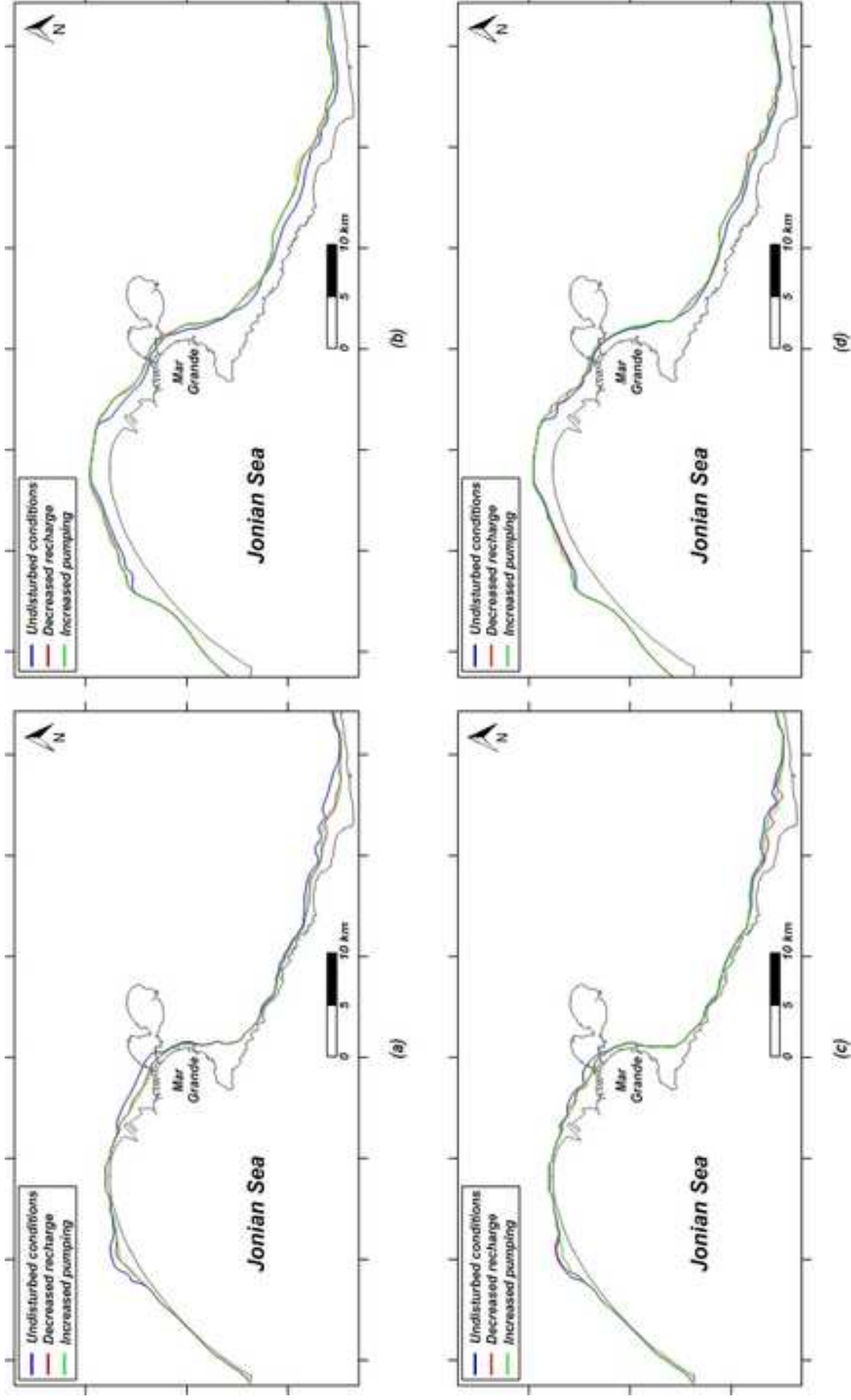


Figure9
[Click here to download high resolution image](#)

